



## Super stable fluorescein isothiocyanate isomer I monolayer for total internal reflection fluorescence microscopy

Title	Super stable fluorescein isothiocyanate isomer I monolayer for total internal reflection fluorescence microscopy
Author(s)	Zarski, Przemyslaw;Ryder, Alan G.
Publication Date	2018-08-27
Publisher	American Chemical Society
Repository DOI	<a href="https://doi.org/10.1021/acs.langmuir.8b02509">10.1021/acs.langmuir.8b02509</a>

DOI: [10.1021/acs.langmuir.8b02509](https://doi.org/10.1021/acs.langmuir.8b02509)

## Super Stable Fluorescein Isothiocyanate Isomer I Monolayer for Total Internal Reflection Fluorescence Microscopy.

Przemyslaw Zarski and Alan G. Ryder.\*

Nanoscale BioPhotonics Laboratory, School of Chemistry, National University of Ireland, Galway, , Galway, H91 CF50, Ireland.

\* Corresponding author: Email: [alan.ryder@nuigalway.ie](mailto:alan.ryder@nuigalway.ie), Phone: +353-91-492943.

**CITATION:** Super Stable Fluorescein Isothiocyanate Isomer I Monolayer for Total Internal Reflection Fluorescence Microscopy. P. Zarski and A.G. Ryder.\* Langmuir, 34(37), 10913-10923, (2018). DOI: [10.1021/acs.langmuir.8b02509](https://doi.org/10.1021/acs.langmuir.8b02509)

**Keywords:** Total Internal Reflection, Microscopy, Fluorescein, Protein, Monolayer, Photobleaching, standard.

**Abstract:** Total internal reflection fluorescence microscopy (TIRFM) is an important method in surface science and for the analysis of surface bound macromolecules. Here, we developed and explored the use of a novel fluorescein isothiocyanate isomer I (FITC)-adsorbed monolayer for alignment and validation of TIRFM measurements and configurations. Aqueous solutions of FITC exist as several different protolytic forms (dianionic, anionic, neutral, and cationic) with each form having different emission characteristics. However, the emission behavior of FITC adsorbed on hydrophilic, hydrophobic, and unmodified glass surfaces at different pH was unknown. TIRFM imaging and spectroscopy were used to study FITC and FITC-labeled bovine serum albumin (BSA-FITC) monolayers generated on three different glass surfaces. Monolayer emission intensity, spectra, and the photobleaching profiles were all dependent on pH and the surface properties of the glass. Very strangely, however, at pH 5.0 on hydrophobic surfaces, the FITC monolayers produced were both bright and apparently unbleachable over ~20 min of imaging (60 s total exposure). During monolayer formation at pH 5.0, we saw clear evidence for concentration-based quenching, indicating high surface coverage. When the monolayer had been rinsed with buffer to remove unbound FITC, we observed an increase in emission intensity during illumination indicative of some form of photoactivated species being present. Eventually, the fluorescence emission stabilized and remained constant for extended periods of time with no evidence of photobleaching. We hypothesize that during the adsorption process (a hydrophobic–hydrophobic interaction) there was conversion to the fluorescent quinoid form of FITC. In contrast, at pH 7.4 and 9.6 on hydrophobic surfaces, FITC monolayers had well-defined, fast photobleaching kinetics (decay to ~50% intensity in 5–10 s). The equivalent BSA-FITC monolayers were slightly brighter, with similar photobleaching kinetics. While the precise mechanism for this unusual behavior is still unknown, all these low-cost monolayers were easily prepared, were reproducible, and can serve as convenient test samples for TIRFM alignment, calibration, and validation prior to undertaking measurements with more sensitive biogenic or biological specimens.

### *Introduction and Background*

Total internal reflection fluorescence microscopy (TIRFM) is an invaluable method for visualizing structures and processes close to the surface of transparent materials.<sup>1</sup> Total internal reflection (TIR) is a relatively simple process: when a light beam travels through a transparent medium of higher refractive index (e.g., glass coverslip,  $n_2$ ) encounters a planar interface with medium of lower refractive index (e.g., aqueous solution,  $n_1$ ) it undergoes TIR for incidence angles  $\theta_i$  greater than a critical angle  $\theta_c$  which is related to the refractive index ratio ( $n_1/n_2$ ) which must be less than one. However, some light will propagate parallel to the surface in the plane of incidence and this propagated energy in the lower refractive index medium is an evanescent wave.<sup>2</sup> The light intensity decays exponentially with distance from the interface yielding very good axial resolution (<200 nm) in the UV-NIR spectral region. This enables researchers to study various interfacial phenomena such as the adsorption of proteins on surfaces<sup>3, 4</sup> and exploring the behavior of engineered surfaces<sup>5</sup> and novel nanomaterials.<sup>6</sup> TIRFM applications often require the accurate quantification of fluorescence emission<sup>7, 8</sup> particularly for protein-surface interaction measurements. However, there are no universal standards.<sup>9, 10</sup> Furthermore, for studying very low-contrast samples, such as fluorophore labelled proteins on surfaces, significant difficulties can be experienced during alignment and in quantifying TIRFM system response under the experimental conditions pertaining to these samples. For instance, the use of fluorescently labelled beads or bulk solution does not replicate adequately the conditions of protein layers being imaged in terms of emission intensity, photobleaching characteristics, and thickness.

Another complication with using fluorophore solutions is that the emission arises from two different populations of fluorophores and three different excitation zones (surface bound layer, evanescent wave zone, and bulk solution excited by scatter). Fluorophores will consist of those surface bound molecules and the free fluorophores in solution, and the photophysical behavior (*i.e.* quantum yield, photobleaching profiles, excitation/emission spectra) will be different. Surface adsorbed fluorophore emission will be influenced by a multitude of specific factors which include: surface chemistry, binding modality, molecular orientation, and inter-probe distances (related to surface coverage). Excitation of both surface and free fluorophores will also be affected by the penetration depth, light scattering, temperature, and other instrumental factors. Ultimately, the detected signal used for calibration is the combination of signals from both bound and free fluorophores excited within theoretically calculated penetration depth, and a contribution from fluorophores in the bulk solution excited by scattered light.

This problem could be eliminated by the use of a fluorescent standard which is only located at the interface and is much thinner than the  $d_p$  of the specific experimental configuration. What is needed are fluorescent monolayers with similar thicknesses and photophysical characteristics to the sample (here proteins) that have similar response level in terms of signal intensity, surface coverage, and photophysical stability. They should be easy to fabricate, inexpensive, safe, useful under a range of different environmental conditions (e.g. surface chemistry, pH, solvent, ionic strength, etc.), and replicate as far as practical the exact

same optical measurement configuration as the experiment. These standards could then be used to confirm that all TIRF alignments and settings (including exposure times) were correctly selected prior to implementing an experiment. Finally, it would be useful if the standard had a reproducible photobleaching rate which should allow users to predict the maximum allowable exposure time in their experiments.

Fluorescein and its derivative, fluorescein isothiocyanate isomer I (FITC) are inexpensive fluorophores widely used in biology. In aqueous solution they are present in several different protolytic forms (di-anionic, anionic, neutral and cationic, Figure S-1, Supplemental Information, SI), depending on the solution pH with each form having different emission characteristics.<sup>11</sup> At near neutral pH (between ~5 and 8) aqueous solutions of fluorescein or FITC contain neutral, mono-anion, and di-anion forms.<sup>12</sup> For fluorescein the three pKa values are in the range 2.00-2.25 (cation/lactone), 4.23-4.4 (neutral/mono-anion), and 6.31-6.7 (mono-/di-anion) and are environmentally sensitive.<sup>11, 13</sup> FITC is very similar with reported pKa values of  $2.05 \pm 0.03$ ,  $4.35 \pm 0.02$ , and  $6.62 \pm 0.01$  (ionic strength of 0.05 M). Changing the physicochemical environment, and placing FITC in a more hydrophobic environment (e.g. CPC micelles) shifts the pKa significantly to:  $1.36 \pm 0.18$ ;  $4.31 \pm 0.01$ ; and  $6.00 \pm 0.01$ .<sup>14</sup> One might expect that FITC adsorption on glass surfaces may induce some change in species composition and that FITC bound to proteins would also undergo some changes because of environmental factors. Furthermore, significant effects will be induced by the close proximity of other fluorophores on the surface because of non-radiative quenching and energy transfer.<sup>15</sup>

We wanted to use fluorophore monolayers as standards for the alignment and validation of TIRFM systems. Here we present a simple methodology for the preparation of both FITC and BSA-FITC monolayers on simple glass substrates. Furthermore, we provide a preliminary photophysical characterization of these monolayers produced on different surface chemistries with different pH environments. These monolayers were very reproducible with well-defined photobleaching properties which can facilitate the selection of the optimum experimental conditions for TIRFM analysis of low contrast and/or weakly fluorescent samples. Finally, one FITC monolayer displayed very strange behavior providing an apparently unbleachable monolayer that may have a wide range of uses (e.g. a nm thick emitter, ) in TIRFM and surface science.

## Material and methods.

**Materials:** FITC isomer I, Bovine Serum Albumin (BSA), Phosphate buffered saline (PBS) tablets (0.01 M phosphate buffer, 0.0027 M potassium chloride, 0.137 M sodium chloride, pH 7.4), and sodium phosphate dibasic were obtained from Sigma-Aldrich. Sulphuric acid 98% was obtained from BDH. Common chemicals like dichlorodimethylsilane, carbonate bicarbonate buffer with azide, citric acid, dimethyl sulfoxide (DMSO) spectroscopic grade, Perdrogen™ 30%

H<sub>2</sub>O<sub>2</sub> (w/w), trichloroethylene A.C.S reagent, 2-propanol Chromasolv<sup>®</sup>, RBS 25 detergent and methanol Chromasolv<sup>®</sup> were all obtained from Sigma-Aldrich. All reagents were used without further purification. All solutions were made up with high purity water (HPW).

For FITC solutions a stock solution of 0.02 g of FITC dissolved in 4 ml of DMSO was prepared, this was then used to prepare buffered solutions with a final FITC concentration of  $1.72 \times 10^{-5}$  M and were prepared fresh each day. To prepare carbonate bicarbonate buffer at pH 9.6, 10 tablets were dissolved in 1 L of HPW. PBS buffer at pH 7.4 was prepared by dissolving 5 tablets in HPW to yield a final concentration of 0.01 M. Citrate/phosphate buffer was prepared by mixing 10.3 ml of 0.2 M Na<sub>2</sub>HPO<sub>4</sub> and ~ 9.7 ml of 0.1 M citric acid for a final pH 5.0. All buffers were used within one week of preparation. BSA-FITC was prepared multiple times (16 reactions) using a method similar to that of Lok *et al.*<sup>16</sup> and purified by column chromatography with sephadex G50 producing a range of BSA-FITC with different label ratios. BSA-FITC batch (#5) used for all monolayer preparation had a FITC:BSA ratio of 2.85:1 as calculated from UV-visible spectra. See SI for further details.

**TIRF instrumentation:** This was based on an inverted Olympus IX81 frame with manual XY stage and motorized Z-axis control. The system was fitted with a triple-line multi-port TIRFM illumination combiner (IX2\_MPITIRTL) with 405, 488, and 561 nm lasers which were coupled using polarization maintaining fibers. Only the 488 nm laser was used in these studies. The system had two ports; one fitted with a wide-field imaging camera Andor EMCCD (iXonTM+, DU897), and the second with an Ocean Optics USB 4000 spectrometer coupled via a multi-mode optical fiber. The objective was an oil immersion Olympus UIS2 PlanApo N 60×1.45 TIRFM with a working distance of 0.1 mm. In general, unless otherwise stated, for all experiments the microscope and the 488 nm laser were switched on three hours prior to making measurements to ensure complete thermal equilibration. All measurements were made with 488 nm excitation at room temperature (21 °C ± 1.5 °C, lab air-conditioning system) and refractive indices of 1.518 (glass), and 1.333 (water) were used for all calculations (unless otherwise stated). All image analysis was done using either the cellR (ver. 3.1, Olympus) or Image J (1.46r, NIH) software. Spectral data were smoothed, normalized, and analyzed using software Origin (ver. 7.5, OriginLab, Northampton, MA, USA).

**Apparatus for monolayer preparation:** The sample system of the apparatus was a flow chamber which could be modified with different surfaces. The top element of the chamber was a sterile bottomless channel slide with a self-adhesive underside to which different substrates can be mounted (sticky-Slide I Luer from ibidi<sup>®</sup>, Figure S-2, SI). This provided a channel 0.1 mm high × 50 mm long × 5 mm wide with an internal volume of 25 μL. The chamber was attached to a solution delivery system designed to flow two different aqueous solutions (buffers and fluorophores) over the different cover slip surfaces at different flow rates. The system (Figure S-3, SI) used a MasterFlex<sup>®</sup> peristaltic pump (model 7712062/60 rpm) which had minimum and maximum flow rates of 0.36±0.01 mL/min, and 2.57±0.04 mL/min respectively. The liquid flow could be switched between two reservoirs one for a buffer wash and the second for the

fluorophore solutions (FITC or BSA-FITC). Here the reservoirs were sterile, 50 ml, polypropylene, centrifuge tubes (Falcon™, Fischer Scientific). All the components of the system were connected via 0.8 mm internal diameter silicone tubing (ibidi®) and assorted plastic Luer valves (World Precision Instruments). Solution flow was operated in two modes: Mode one was flowing buffer solution from reservoir 1, through the flow chamber, and then to waste. Mode 2 was a closed cycle flow of the fluorophore from reservoir 2, through the chamber and back to the same reservoir. The first mode provided continuous flow of fresh buffer solution which is required for rinsing the flow chamber, and mode two provided continuous flow of fluorophore solution required during monolayer formation.

**Substrate Surface Preparation:** Borosilicate microscope cover slips N#1.0 (VWR International) were used throughout. Hydrophilic surfaces were prepared by first sonicating the slides for 1 hr. in a 2 % (v/v) solution of alkaline RBS 35 detergent. They were dried in air at room temperature for ~ 15 min and placed in special cylindrical coverslip glass holders and soaked for 3 hours in piranha solution (3:7, v/v, H<sub>2</sub>O<sub>2</sub>:H<sub>2</sub>SO<sub>4</sub>). The slides were then rinsed three times with HPW and then sonicated for 1 hour in HPW, before a final rinsing and storage in fresh HPW until use. This treatment gave a hydrophilic surface with a contact angle for water-based solutions that was close to zero. The hydrophilic surface is believed to consist of a nm thick, hydrated oxide layer with a large number of silanol groups which are amphoteric. This yields a surface that has both proton acceptors and donors which produces a point of zero charge close to pH 3.0.<sup>17</sup> At neutral pH these hydrophilic surfaces should be negatively charged and potentially could adsorb cationic species. The unmodified surfaces were cover slips that were used as received apart from using canned air to remove any surface dust.

Hydrophilic surfaces were converted to hydrophobic surface substrates as follows. Slides were removed from the HPW and then dried overnight in air at 80 °C before being sonicated in a 2% solution of dimethyl-dichlorosilane in trichloroethylene for 3 hours before rinsing with trichloroethylene ×3, methanol ×3 and finally HPW. Hydrophobic surfaces were stored in methanol at room temperature prior to use. The methylation process gave a surface covered with methyl groups covalently bound to the glass surface by silicone-oxygen bonds.<sup>18</sup> The hydrophobicity and hydrophilicity were qualitatively assessed by measuring water contact angles<sup>19</sup> with a digital camera and an in-house assembled rig. The contact angles (triplicate measurements) were 5.8±4.1, 54.6±2.7 and 86.7±4.5 degrees for the hydrophilic, unmodified, and hydrophobic surfaces, respectively.

**Monolayer Preparation:** The reservoirs (50 mL volumes for the fluorophore solutions) were first filled with a buffer solution of specific pH (5.0, 7.4, or 9.6) and solutions of FITC ( $1.72 \times 10^{-5}$  M) or BSA-FITC ( $3.63 \times 10^{-6}$  M) in the same buffer respectively. All buffer solutions used in the experiment as well as those for FITC solution preparation were filtered using a vacuum driven sterile filter cup with a 0.22 μm pore size Stericup™ Express Plus membrane (Millipore). Solutions were partially degassed using an ultrasonic bath. To begin fluorophore adsorption, the flow chamber was allowed to equilibrate with a constant flow (0.36 ml/min) of the appropriate

buffer for 5 minutes. Then the FITC (or BSA-FITC) solution was introduced for a 30-minute incubation time (closed circuit flow, 0.36 ml/min). After this incubation period, the fluorophore solution was replaced by a constant flow (0.36 ml/min to waste) of fresh buffer for 10 minutes to remove excess / unbound fluorophore.

**Measurement Procedures:** Two types of measurement were made on the TIRFM setup: first a wide-field image of the surface from which a total integrated fluorescence intensity was calculated, and second emission spectra (uncorrected for instrument response) were collected using the Ocean Optics USB 4000 spectrometer. Since these used opposite ports, it was easy to collect both imaging and spectral data from the same sample, however, different regions of interest (ROI) were used for each type of measurement because of photobleaching. The fluorescence emission intensity over the field of view (FOV) was measured by imaging during the buffer solution wash (0-5min), fluorophore bulk solution incubation (5-35 min), and FITC/BSA-FITC monolayer phase (45-65 min).

For the first five minutes five images were collected to confirm that the flow system was not fluorophore contaminated from improper cleaning or via a leak from the second circulation system containing the fluorophore or protein solution. After these measurements, buffer flow ceased and FITC (or BSA-FITC) solution was introduced to the flow chamber for a 30 minutes incubation period. To monitor monolayer formation, six images were taken at five-minute intervals. After incubation the fluorophore supply was switched off and a 10-minute buffer wash implemented to remove any unadsorbed fluorophore/protein solution from the surface. After flushing, the peristaltic pump was turned off and imaging/spectral measurements of the monolayers were undertaken. For 20 minutes the monolayers were imaged ( $\lambda_{ex}=488$  nm) and 240 images each with an exposure time of 250 ms were taken (total exposure time of 60 seconds). Each image had a  $\sim 0.02$  mm<sup>2</sup> FOV, and the average emission intensity was calculated across the full FOV for each image. For the spectroscopic measurements a new ROI was selected, and the exposure time was set to 1.5 sec with a 30 sec. total integration time per spectrum. For the three different glass surfaces (hydrophilic, unmodified, and hydrophobic), FITC and BSA-FITC monolayers were prepared in triplicate at pH 5.0, 7.4, and 9.6.

## Results and Discussion.

**FITC Monolayers:** The nine different fluorophore-surface combinations (3×pH, 3×surface chemistry) for FITC and BSA-FITC, produced significantly different responses as might be expected.<sup>13</sup> In each case TIRF imaging showed that the emission intensity varied very significantly according to surface (related to degree of coverage) and that the hydrophilic surfaces were mostly unsuitable (Figure 1 and SI). During the buffer wash control phase ( $t=0-5$  minutes), in all cases, this signal was  $< 500$  a.u. (arbitrary units), which was the average pixel

intensity from the 512×512-pixel image. This was remarkably consistent across all samples, which were prepared in triplicate on different days (for each pH/surface/monolayer combination) and over approximately 18 months from the complete set of data presented here. We note also that the standard deviation in this signal was less than 0.5% across the image (Figure S6/7) which indicated high system stability.

The hydrophilic surface data (Figure S-8, SI) served as control measurements and provide data about to the emission intensity of the freely diffusing fluorophores in the bulk solution above the surface because there is no evidence for any fluorophore adsorption (signal before and after incubation phase is the same) and there is no upward trend in the plot. The hydrophilic surface consists of a nm thick hydrated oxide layer with a large number of silanol groups<sup>17</sup> that resists adsorption. Thus, we can be confident that the bulk FITC solution has an intensity of ~1700 a.u. at pH 9.6 and ~1400 a.u. at pH 7.4, so monolayers on the hydrophobic surfaces at these pH values contribute a maximum signal of ~1700 a.u. and ~2900 a.u. respectively. For unmodified surfaces the fluorescence intensity contribution from adsorbed FITC during incubation was very low ~200 a.u. at pH 9.6 and ~700 a.u. at pH 7.4. After the buffer wash, the monolayers only had peak intensities above baseline of ~400 and 350 au respectively. We can conclude therefore that the unmodified surfaces were unsuitable for preparing fluorescent monolayers.

During incubation ( $t = 5\text{--}35$  minutes) for the hydrophobic and unmodified surfaces we observed a large increase in fluorescence intensity which comprised of signal from both the surface bound and freely diffusing FITC in the layer excited by the evanescent wave ( $d_p \sim 200$  nm) just above the surface. The maximum intensity achieved during incubation was determined by two factors: first, the FITC forms present (most important) and second the degree of surface coverage. The profile in this phase gave an indication of the rate of monolayer formation which was determined by surface chemistry and the protolytic forms present (all other conditions being identical). At these pH values, FITC (like fluorescein) exists as a mixture of neutral, mono-anion, and di-anion forms, all of which will have different quantum yields,<sup>11, 14, 20</sup> thus changes in monolayer emission intensity may arise from the absorption of specific FITC forms onto different surfaces. We compared the emission spectra of both FITC and fluorescein and confirmed that they followed the same behavior and had almost identical spectra (Figure S-5, SI). The major FITC form present in pH 5.0 solution was the mono-anion, whereas the di-anion form was more prevalent at pH 7.4 and 9.6. The reported quantum yields of fluorescein were ~0 (neutral form),  $\sim 0.37 \pm 0.2$  (mono-anion), and  $\sim 0.93$  (di-anion) in buffer.<sup>11</sup> However, the neutral form can exist as three different isomers: quinoid, zwitterion, and lactone which in solution were reported to be present in a 15:15:70 ratio.<sup>13</sup> Only the quinoid is fluorescent with a quantum yield of  $\sim 0.29$  which was comparable to the mono-anion. We assumed that a similar trend occurred with FITC, however, there was very little literature data about either fluorophore on glass surfaces. Overall monolayer formation at pH 7.4/9.6 on unmodified and hydrophobic surfaces followed fairly standard adsorption models as have been described in the literature.<sup>21, 22, 23</sup> A

slight decrease in emission intensity was observed for the unmodified surface during the latter stages of incubation and this was probably due to photobleaching of the adsorbed monolayer.

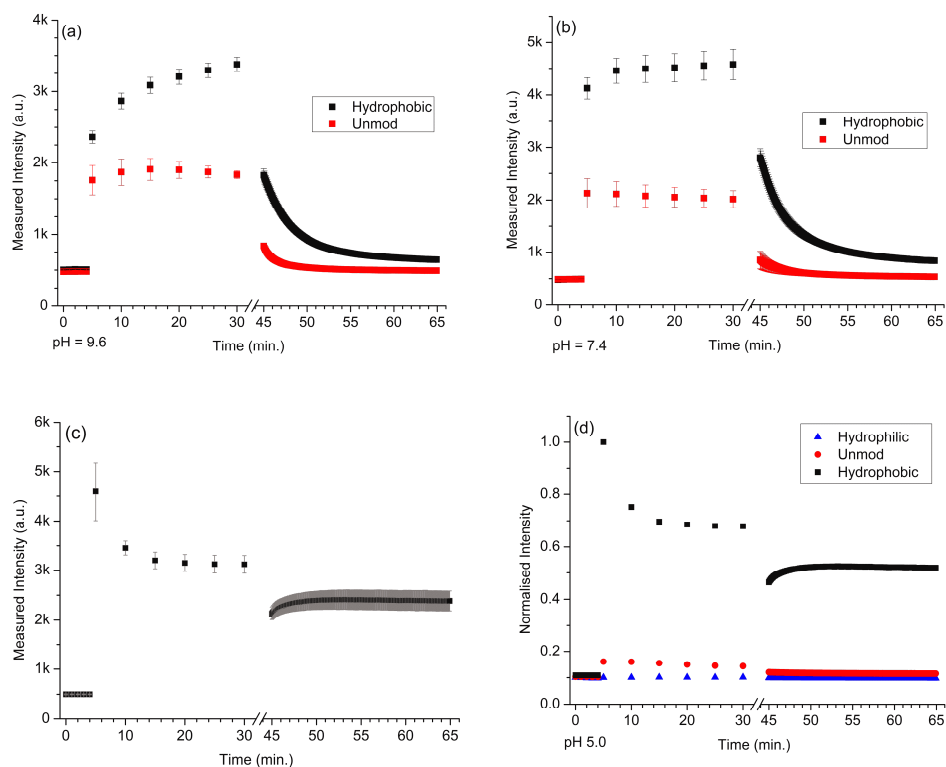


**Figure 1:** Plots emission intensity versus time showing FITC monolayer formation and photobleaching at different pH on three different surfaces: hydrophobic and unmodified surfaces at pH 9.6 (a) and 7.4 (b); and hydrophobic surfaces at pH 5.0 (c). Panel (d) shows the normalized intensity profiles for the surfaces at pH 5.0 (Data from the other hydrophilic surfaces are shown in the SI). Emission intensity calculated from TIRFM widefield images and the error bars represent the variation from measurements made on three different samples.

After incubation, the buffer rinse ( $t=35\text{--}45$  minutes) removed unbound FITC and then when imaging recommenced (static buffer conditions) it was noted that significantly lower signal intensities were measured (decreases of  $\sim 45\%$  for hydrophobic and  $\sim 60\%$  for unmodified), which originated only from the monolayer. Emission intensities were approximately three times more intense from hydrophobic monolayers (at pH 7.4 and 9.6) compared to the unmodified glass surfaces (Figure 1a/b) which suggested that in both cases surface coverage was much greater on these surfaces assuming that the protolytic population distribution did not change between bulk and surface. During imaging of the formed monolayers (15 minutes) all pH 7.4/9.6 monolayers rapidly photobleached (Figure 1) at slightly different rates. Overall the pH 7.4 / hydrophobic surface combination gave the brightest monolayers with normal photobleaching

behavior, probably due to the fact that at this pH, binding was relatively strong and the quantum yield of the adsorbed protolytic forms (mostly mono- and di-anion) was relatively large.

Hydrophilic surfaces at pH 5.0 during the incubation phase ( $t = 5\text{--}35$  minutes) showed virtually no emission (Figure 1d, Figure S-8, SI). At this pH FITC in solution was expected to be present as the mono-anion with a small, but significant contribution of neutral form,<sup>11, 13, 24</sup> and cuvette measurements showed that this was the case (Figure S-5, SI). Since emission from the bulk solution during TIRF measurements was very weak this indicated that either there was only a small amount of the anionic form present or there was a boundary layer preventing free FITC approaching the evanescent wave zone. The equivalent unmodified surface shows weak and reducing emission during the incubation period. It was possible that a boundary layer generated by surface bound water<sup>25, 26</sup> was present which could prevent mono-anion adsorption onto the glass surface. However, any water bound layer was not likely to extend outwards more than  $1\text{--}2\text{ nm}$ <sup>27</sup> which means that FITC could still be present within the evanescent excitation zone.

Irrespective of which case pertained above for the hydrophilic controls, any emission from hydrophobic surfaces at pH 5.0 must involve different protolytic forms. For the unmodified surfaces, emission intensity was slightly raised above baseline during incubation, indicating that some changes had occurred. However, for the hydrophobic surface, there was very strong emission which meant that we had an adsorbed emitting species of a different protolytic form compared to the bulk. The shape of the intensity plot during the incubation phase was also somewhat similar to the TIRF plots reported by Robeson and Tilton for FITC-RNase A adsorbed to polystyrene,<sup>28</sup> which indicated the presence of concentration quenching. This concentration quenching during incubation supports this view that there was a high surface coverage and thus many FITC molecules located close together within the Förster radius which was reported to be  $\sim 50\text{ \AA}$ .<sup>29</sup> After incubating for  $\sim 10$  minutes, the adsorbed layer displayed a constant emission intensity (of  $\sim 3100$  a.u.).

It is not known at this stage how the ratio of protolytic forms and quantum yields might change on adsorption to glass surface. However, it has been reported that for fluorescein (and several derivatives) in micelles, hydrophobic interactions promoted the neutral quinoid form formation,<sup>30</sup> whereas in solution the non-fluorescent lactone was favored.<sup>13</sup> We suspect that on adsorption, neutral FITC adopted the quinoid structure and therefore was switched on, producing significant emission, and that this process was driven by hydrophobic-hydrophobic interactions. It was also possible that the fluorescent mono-anion could also adsorb and this was demonstrated by Maeda and co-workers who used vibrationally electronically doubly resonant sum-frequency generation (DR-SFG) spectroscopy to study FITC layers on platinum.<sup>12</sup> They concluded from the spectral and modelling data that their adsorbed monolayers comprised of both anion and neutral forms only, of which only the anionic form emitted. However, it should be noted that since their measurements were made on a metal surface, quenching and surface plasmon effects may also have a large effect on the emission properties. Furthermore, and quite surprisingly, this

monolayer was extremely photostable and we did not see any evidence of photobleaching. This was not an isolated result and this behavior was replicated multiple times over several years with dozens of samples. The emission intensity of the formed monolayer was also relatively high ~2500 a.u. indicating good surface coverage of species with relatively high quantum yield.

**Monolayer photo-stability:** When we assessed FITC monolayer stability on hydrophobic surfaces we observed that at pH 7.4 and 9.6 the monolayers bleach relatively quickly (from  $t > 45$  minutes) during imaging, on the timescale of minutes under the conditions used here. These non-single exponential photobleaching profiles were similar to that reported for FITC adsorbed on silica surfaces<sup>31</sup> and agreed with the simulations and theory proposed by Song and co-workers.<sup>32</sup> In these cases, bleaching is due to a combination of processes involving the triplet state, one a D-D (dye-to-dye) and the other a D-O (dye-to-oxygen).<sup>33</sup> For these monolayers we assumed that there was a relatively high surface coverage so that the D-D process should dominate. Bleaching from the hydrophobic surfaces was both slower and different from that measured from the unmodified surfaces particularly at pH 9.6 (Figure 2a) which was attributed to differences in surface protolytic forms and concentrations. Normalized emission spectra (Figure 3a/b) showed small spectral differences indicative of these population differences. Bleaching profiles were very reproducible (Figure S-6, SI) and thus can provide a convenient, inexpensive, easy to prepare test substrate for fine-tuning TIRF alignment, collection efficiency, and imaging parameters to minimize photobleaching prior to undertaking experiments with expensively labelled biological targets.

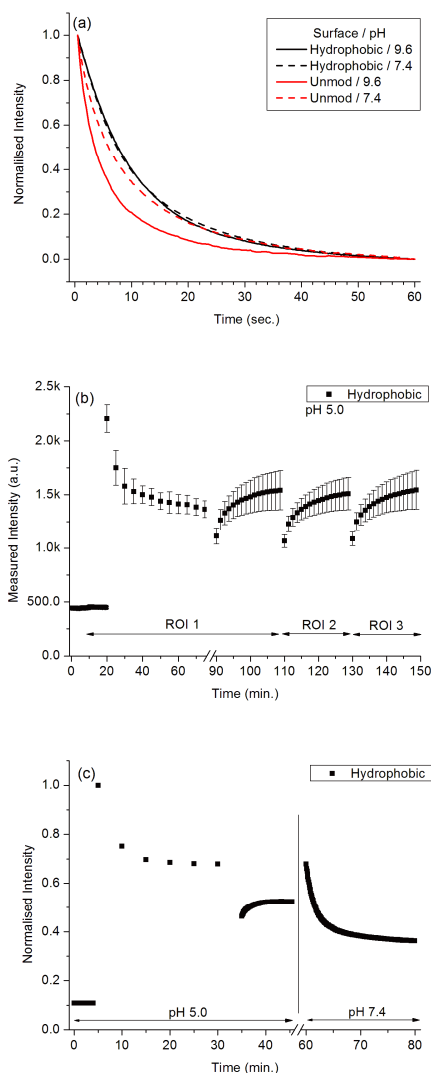


**Figure 2:** (a) Normalized photobleaching curves showing the relative decrease in FITC fluorescence as a function of exposure time (for a total of  $240 \times 250$  ms exposures) for the hydrophobic and unmodified surfaces; (b) Fluorescence recovery measured at different ROI's for the pH 5.0 FITC monolayer on a hydrophobic surface. Error bars were calculated from triplicate measurements on different samples; (c) Demonstration of hydrophobic monolayer surface population change with pH change from 5.0 to 7.4.

The pH 5.0 monolayer under our imaging conditions showed no photobleaching and was dramatically more stable than any of the other monolayers produced. According to the well-established bleaching mechanisms for fluorescein<sup>32</sup> and FITC<sup>28</sup> one would expect both D-D (*i.e.* concentration quenching) and D-O mechanisms to operate here. We note also that for the pH 5.0/hydrophobic surface immediately after the buffer wash, fluorescence intensity decreased to  $\sim 68\%$  of the  $t=30$  min value, before recovering to  $\sim 77\%$  (Figure 1c/d). This looked like

fluorescence recovery after photobleaching (FRAP) involving triplet state recovery rather than a diffusion based processes,<sup>34</sup> however, the long-time delay (~10 minutes) between measurements here rule that explanation out. Recovery of FITC emission on surfaces has also been reported previously where alkaline washes regenerated the anionic fluorescent forms.<sup>12, 35</sup> We propose that something similar occurred here with a surface equilibrium between emitting (i.e. the quinoid form) and dark forms of neutral FITC (and possibly mono-anion) present. The initial change to buffer solution removed loosely bound FITC, causing the initial intensity drop recorded at  $t=45$  minutes from this initial surface population (Figure 1d). As illumination progresses we first get an increase in intensity, followed by a stable emission (Figure 2b) which could be attributed to one of two processes. One possibility is the photoactivation of a surface bound species during the initial irradiation process causing the increased emission. An alternative explanation could be that photobleaching during this initial illumination phase could decrease the rate of concentration quenching by the increased average distances between emitting fluorophores, similar to that reported for FITC-RNase.<sup>28</sup> However, one might expect this process to ultimately also produce an eventual decrease in emission as more fluorophores were bleached, and this was not observed during the illumination times used here. Interestingly, if the buffer above one of these anomalous surfaces was changed to pH 7.4 the emission properties change dramatically, presumably via the generation of more dianion. Monolayer emission intensity increased and was then rapidly photobleached similar to the pH 7.4 monolayers (Figure 2c), however, it did not bleach back down to baseline, which indicated that only the dianion was bleached and that a layer of the photostable FITC form remained on the surface. The precise basis for this behavior is unknown, but probably involves several interlinked excited state processes and requires further detailed investigation which is outside the scope of this study (and our experimental facilities). However, and more importantly, this was a very reproducible effect, across different ROIs and samples, making this system a useful TIRF standard for instrument alignment, focus adjustments, and optimization of illumination/excitation settings. As the emission intensity does not bleach during extended illumination and is nearly constant after the initial increase, it allows one to effectively test a variety of optimizations and alignments with the same sample and same focus point (at nm precision). This is particularly important in the context of optimizing collection efficiency for biological experiments where photobleaching can be very problematical.

**Spectral Analysis:** The normalized fluorescence emission spectra of the FITC monolayers (Figure 3) on the hydrophobic and unmodified surfaces were not quite identical which was indicative of similar emitting species being present but with different concentrations at every pH. In solution the FITC solutions at these pH's were virtually identical (Figure S-12, SI) whereas the monolayer spectra (Figure 6b) were slightly red-shifted. Overall these spectra suggested that on the surfaces the emitting species populations were similar and mostly originated from the dianion with a small mono-anion contribution.<sup>11, 13, 14, 24</sup> In contrast, the very weak emission spectra recorded from the hydrophilic surfaces closely resembled the spectra recorded from the

buffer solutions (Figure S-7, SI), which is further proof that stable FITC monolayers did not form on these surfaces.

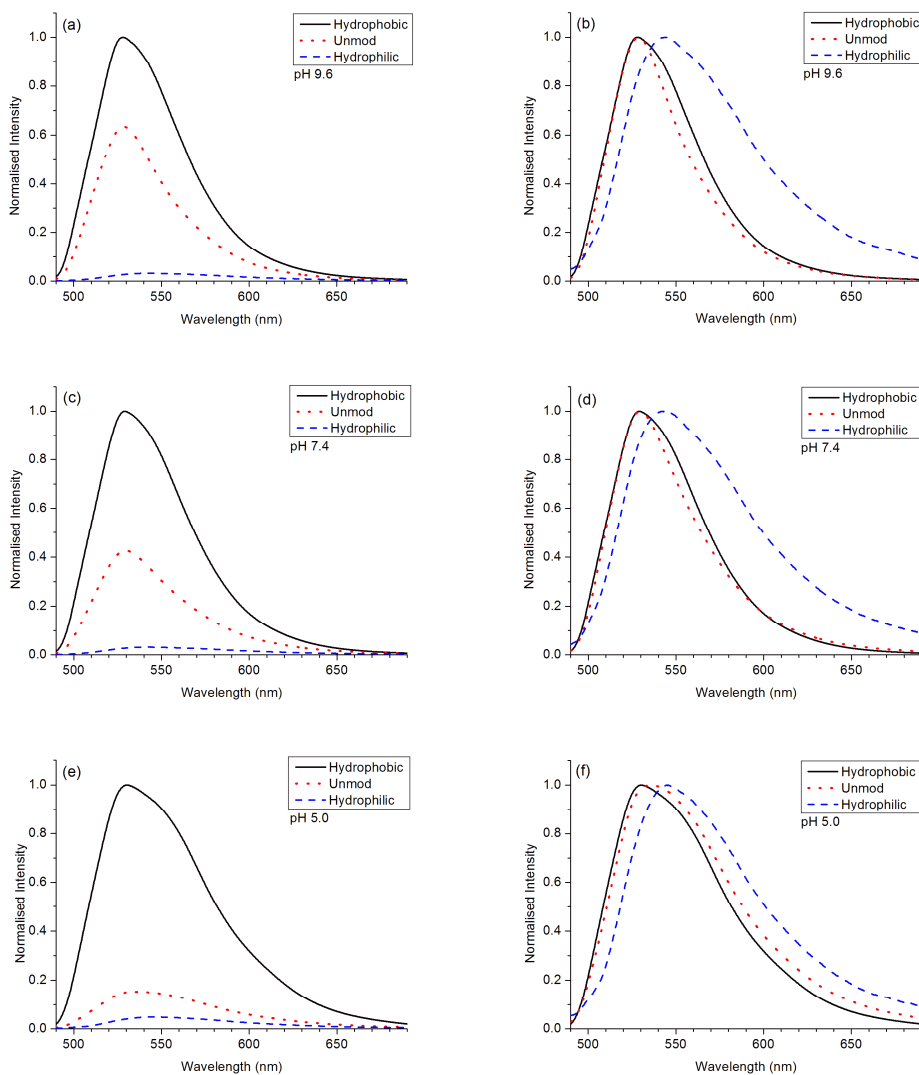


**Figure 3:** Normalized fluorescence emission spectra of FITC monolayers on different surfaces at: *(a/b)* pH = 9.6; *(c/d)*: 7.4; and *(e/f)*: 5.0. The spectra on the left were normalized to the maximum intensity of the hydrophobic surface monolayer spectra. Spectra on the right were normalized to the point of maximum intensity of each individual spectrum. All spectra were uncorrected for instrument response. The measured spectra are shown in the SI (Figures S9-11).

In all cases there was a small but significant spectral red shift in the band maximum (from ~3 nm at pH 9.6 to ~ 5 nm at pH 5.0) and in the shape of the spectra (see also Figure 6b)

on going from bulk solution to monolayers. This redshift could be caused by three factors: first, a change in protolytic form distribution on surface adsorption, second, the close proximity of fluorophores resulting in energy migration,<sup>29</sup> and third, the change in fluorophore environment when surface adsorbed. For hydrophobic surfaces, the red-shift at pH 9.6 was the smallest which indicated similar species on the surface and in solution which that was mostly the dianion with a contribution from the mono-anion. At pH 7.4, the larger red-shift indicated a large change in the di-anion/mono-anion distributions and suggested a greater mono-anion surface population because mono-anion emission extends further to the red.<sup>11, 13</sup> For pH 5.0, concentration quenching evident during incubation phase also contributed to the more significant red-shift. The pH 5.0 bulk solution spectrum (SI, Figure S-5) was very similar to mono-anion emission, however, it has been reported that the fluorescein quinoid form has a similar emission spectrum to the mono-anion.<sup>13</sup> It was also interesting to note that during the spectral measurements with different exposure times (Figure S-9, SI) the spectral shape did not change for the pH5/hydrophobic FITC monolayers in contrast to the other monolayers (Figures S-10 & S-11) where there was a noticeable red-shift in the spectra as a consequence of photobleaching. This is further evidence for a stable surface population of emitting species.

**BSA monolayers:** For BSA-FITC relatively bright, reproducible monolayers were generated at all pH values (Figure 4 & 5) with the pH 9.6 layers on hydrophobic surfaces being the brightest and the quickest to form. The intensity of the monolayer emission in all cases after the buffer wash ( $t > 45$  minutes) was much higher compared to the FITC case (Figure 1a/b). The intensity was  $\sim 2.5\times$  and  $1.25\times$  greater at pH 9.6 and 7.4 respectively and this could be attributed to the much stronger protein adsorption and the minimization of concentration quenching. However, the most stable monolayers were generated at pH 5.0 which was close to the isoelectric point for BSA (Figure 4). It was noticeable that none of the BSA monolayers displayed similar behavior to that of the FITC hydrophobic/pH 5.0 monolayers (Figure 1c). The weakly fluorescent BSA monolayer formed on the hydrophilic surfaces at pH 5.0 was indicative of the greater adhesion properties of proteins.

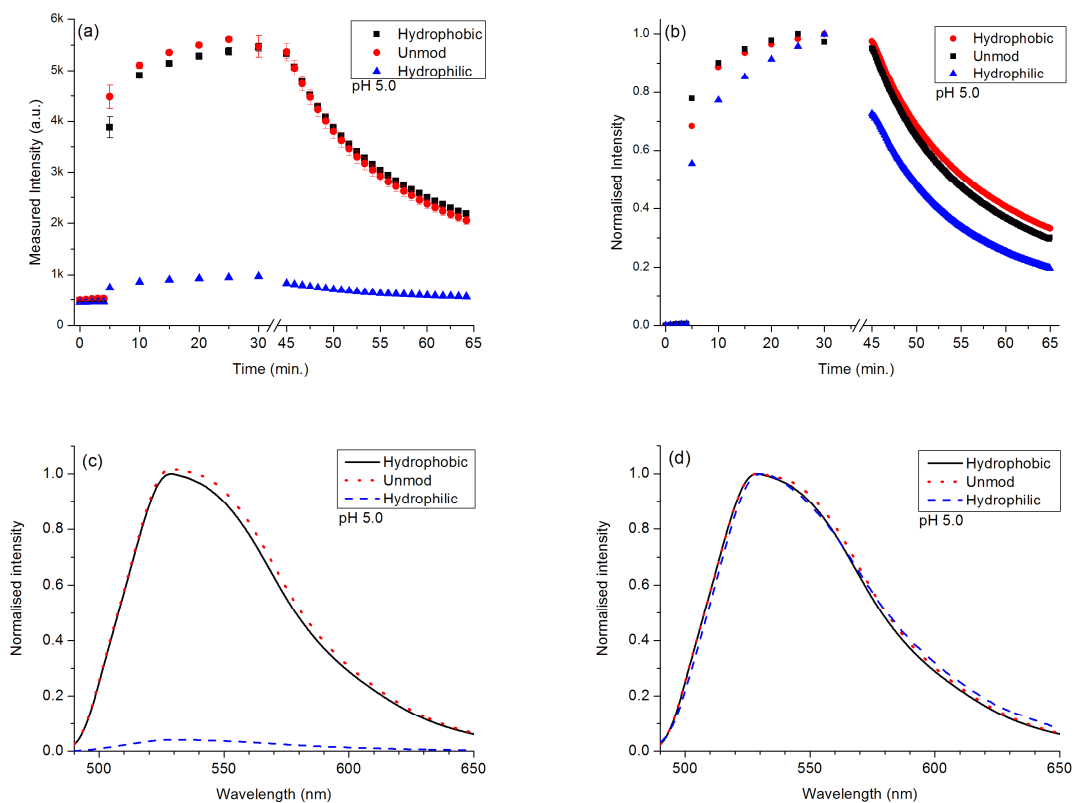


**Figure 4:** Emission intensity versus time showing monolayer formation and photobleaching of the BSA-FITC monolayers at pH 5.0 on the three different surfaces (a). Panel (b) shows the normalized (to maximum value of curve) adsorption kinetic plots illustrating the differences between layers; Raw as recorded (c) and the normalized (d) emission spectra of BSA-FITC monolayers at pH 5.0.

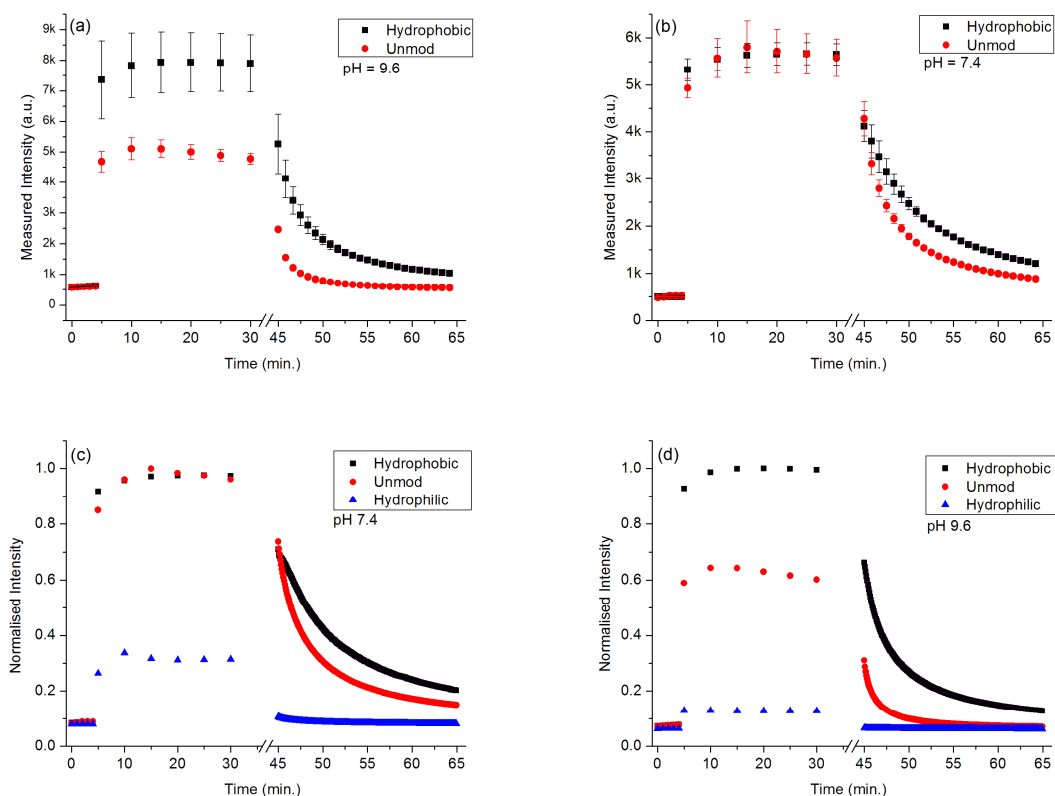


**Figure 5:** Plots of emission intensity (from TIRFM images) versus time showing the formation and photobleaching kinetics for the BSA-FITC monolayers at pH 9.6 (a) and 7.4 (b) for the hydrophobic and unmodified surfaces (the hydrophilic surfaces are shown in the SI). The error bars are for triplicate measurements from three different samples. Normalized plots (to the most intense measurement) for pH 9.6 (c) and pH 7.4 (d) BSA-FITC monolayers.

The second difference between FITC and the BSA-FITC monolayers was the superior resistance to photobleaching at pH 7.4 on the hydrophobic surfaces (Figures 2/5 and Figure S-14, SI). This was due to two factors: the fact that FITC when bound to the BSA is likely to be sterically protected, and there was a different population of protolytic forms present when bound to protein as was clear from the emission spectra (Figure 6). The FITC:BSA labelling ratio of 2.85:1 probably results in a FITC:FITC distance of  $\sim 53$  Å, based on the data and analysis of Hungerford *et al.*<sup>29</sup> At these labelling ratios energy migration between FITC fluorophores in each BSA protein were significant which probably reduces intensity somewhat, but this might be one of the reasons why the photobleaching in BSA-FITC monolayers was reduced. However, the effect was localized to individual BSA molecules and it was unlikely that there was much inter-BSA energy transfer due to the large size of BSA and the relatively low labelling ratio used here.<sup>28</sup>

**DOI:** [10.1021/acs.langmuir.8b02509](https://doi.org/10.1021/acs.langmuir.8b02509)

At pH 5.0 BSA-FITC monolayers had very different behavior and spectral response compared to the FITC monolayers and this was a result of the FITC being located within the BSA and not directly attached to the surface. Spectrally, pH 5.0 BSA-FITC monolayers were virtually the same for all three surfaces apart from the intensity (Figure 3e/f and Figure S-13e/f) which indicated that the BSA surface conformation was very similar in all cases and that the only significant difference was the degree of surface coverage. Band fitting of the emission curve indicated (data not shown) that there were at least two bands present which might suggest emission from both neutral and mono-anion FITC.

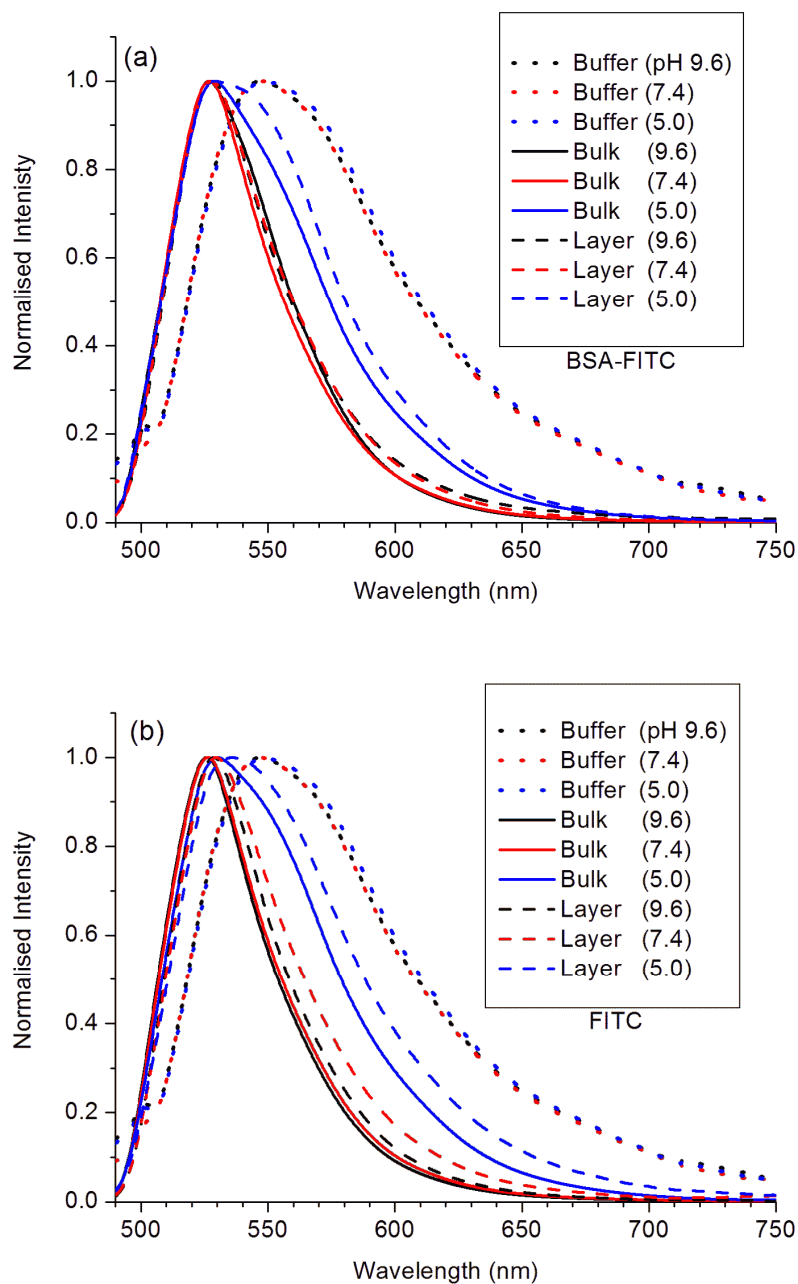


**Figure 6:** Overlaid, normalized fluorescence emission spectra at different pH of buffer (dotted lines), bulk solution (solid lines), and the adsorbed monolayers on hydrophobic surfaces (dashed lines) for **(a)** BSA-FITC and **(b)** FITC.

At pH 9.6 the normalized spectra for the hydrophobic and unmodified surfaces (SI, Figure S-13) overlap perfectly and the emission was strong indicated that the monolayer contained mostly the

dianion form. However, this layer rapidly photobleached making these unsuitable as standards. When the pH was changed to 7.4, the bulk and hydrophobic monolayer spectra were very similar (there was a small red-shift), which indicated that the surface and solution populations of protolytic forms were very similar. However, there was a noticeable difference at pH 7.4 between the unmodified and hydrophobic surfaces with the hydrophobic monolayer having a noticeable extension into the red (SI, Figure S-13). BSA at pH 7.4 (10 mM phosphate buffer) on hydrophobic surfaces is known to have a side-on surface orientation<sup>36</sup> and a stronger interaction which may change its conformation compared to the unmodified surface where the attractive forces were less. This appears to cause less emission from the dianion and a more mono-anionic character in the emission.

We can be confident that for both BSA-FITC and FITC monolayers have been generated and that these will have nm thicknesses of <20 nm for the BSA-FITC and 2-3 nm at most for the FITC. There are several reasons for this: First, the fluorophore concentrations used for were very low  $1.72 \times 10^{-5}$  M for FITC and  $3.63 \times 10^{-6}$  M (241 ppm) for BSA-FITC (50 mL volumes of each) making it very unlikely that multilayers were being generated particularly since the conditions were very mild. Lassen *et al.* reported that for various polymer and plasma treated surfaces 100 ppm HSA-FITC solutions yielded 4-5 nm thick monolayers whereas for more concentrated 400 ppm solutions a thicker ~15 nm layer was formed.<sup>37, 38</sup> The BSA-FITC concentration used here were in between these values and we expect that the BSA will have adsorbed in an end-on configuration generating the thicker layer.<sup>39, 40</sup> Second, the preparation conditions employed here were similar to those reported by Phan *et al.*,<sup>41</sup> and other authors,<sup>16, 42</sup> all of whom report nm layer thicknesses in the nm size range measured by ellipsometry, atomic force microscopy,<sup>43</sup> or other methods.<sup>42, 44</sup> For FITC the low concentration and relatively short incubation times, coupled with no obvious mechanism for an alternative reactions is sufficient evidence for monolayer formation and thus a thickness of 2 nm or less.

## Conclusions:

Reproducible FITC and BSA-FITC monolayers were easily generated on hydrophobic and unmodified glass surfaces which were sufficiently photostable for TIRF setup and validation, and the collection of emission spectra using relatively simple, uncooled multi-channel fiber optic connected spectrometers. Apparently unbleachable FITC monolayers at pH 5.0 on hydrophobic surfaces provided a very stable substrate which can be used to verify optical collection efficiency of different TIRFM configurations. During imaging with 488 nm illumination the layers were photostable for >15 minutes and thus offer a low-cost alternative to expensive photostable fluorophores such as the Alexa family.<sup>45</sup> The source of this unique emission seems to originate from the combined emission of the neutral quinoid and mono-anion forms, however, the precise mechanism of both the increased emission during initial illumination and photostability is

DOI: [10.1021/acs.langmuir.8b02509](https://doi.org/10.1021/acs.langmuir.8b02509)

unknown. Some form of excited state energy transfer between the two forms might explain this however, further, more detailed, advanced photophysical studies are needed.

We also showed that relatively stable and bright, FITC monolayers were easily prepared on hydrophobic glass surfaces at pH 9.6 and 7.4. These had well-defined photobleaching profiles and provide a convenient method for assessing total illumination time available during TIRFM experiments. These monolayers can thus be used as a simple substrate for optimizing alignment and/or image acquisition parameter setup prior to imaging unstable samples. Another FITC monolayer advantage was that they were quicker and easier to prepare and use than fluorophore labelled proteins. It was relatively easy, but time-consuming to prepare reproducible BSA-FITC monolayers, however, the quality and reproducibility of the layers is very sensitive to multiple factors. First, BSA-FITC labelling ratio can affect both fluorescence emission<sup>29, 46</sup> and adhesion properties.<sup>46</sup> Thus, for use as a reproducible standard, required very careful labelling, purification, characterization, and handling. Here we used a single batch of labelled BSA-FITC, ensuring reproducible layer formation and emission properties with reasonable photostability. Compared to using fluorescent nanoparticles or microbeads these monolayers offer an alternative which is guaranteed to be much thinner, is adhered to the surface, and has similar emission properties to labelled proteins and /or cells being investigated using TIRFM.

In conclusion, these monolayers are robust control measurements for TIRF system performance validation prior to undertaking for measurements with less photostable biological samples. However, more detailed photophysical study of the “*unbleachable*” hydrophobic/pH5 FITC monolayer system is required to provide an unambiguous explanation for its very high photostability.

### Supplemental information available:

The Supporting Information is available free of charge on the [ACS Publications website](https://doi.org/10.1021/acs.langmuir.8b02509) at DOI: [10.1021/acs.langmuir.8b02509](https://doi.org/10.1021/acs.langmuir.8b02509).

### Acknowledgments

This research was conducted with the financial support of the Irish Research Council (#RS/2012/615, funding to PZ) and Science Foundation Ireland (grant #02/IN.1/M231S1 to AR) which funded the TIRF system used here.

### References:

1. Fish, K. N. Total internal reflection fluorescence (TIRF) microscopy. *Current protocols in cytometry / editorial board, J. Paul Robinson, managing editor ... [et al.]* **2009**, Chapter 12, Unit12.18.
2. Axelrod, D. Chapter 7 Total Internal Reflection Fluorescence Microscopy. In *Methods in Cell Biology*, Dr. John, J. C.; Dr. H. William Detrich, III, Eds.; Academic Press, 2008; Vol. Volume 89, pp 169-221.

3. Robeson, J. L.; Tilton, R. D. Spontaneous reconfiguration of adsorbed lysozyme layers observed by total internal reflection fluorescence with a pH-sensitive fluorophore. *Langmuir* **1996**, *12* (25), 6104-6113.
4. Petrash, S.; Cregger, T.; Zhao, B.; Pokidysheva, E.; Foster, M. D.; Brittain, W. J.; Sevastianov, V.; Majkrzak, C. F. Changes in protein adsorption on self-assembled monolayers with monolayer order: Comparison of human serum albumin and human gamma globulin. *Langmuir* **2001**, *17* (24), 7645-7651.
5. Koo, J.; Erkkamp, M.; Grobelny, S.; Steitz, R.; Czeslik, C. Pressure-Induced Protein Adsorption at Aqueous-Solid Interfaces. *Langmuir* **2013**, *29* (25), 8025-8030.
6. Caporizzo, M. A.; Sun, Y. J.; Godman, Y. E.; Compostot, R. J. Nanoscale Topography Mediates the Adhesion of F-Actin. *Langmuir* **2012**, *28* (33), 12216-12224.
7. Gaigalas, A. K.; Li, L.; Henderson, O.; Vogt, R.; Barr, J.; Marti, G.; Weaver, J.; Schwartz, A. The development of fluorescence intensity standards. *Journal of research of the National Institute of Standards and Technology* **2001**, *106* (2), 381.
8. Waters, J. C. Accuracy and precision in quantitative fluorescence microscopy. Rockefeller University Press, 2009.
9. Young, I. T. Quantitative microscopy. *IEEE Engineering in Medicine and Biology Magazine* **1996**, *15* (1), 59-66.
10. Model, M. A.; Burkhardt, J. K. A standard for calibration and shading correction of a fluorescence microscope. *Cytometry* **2001**, *44* (4), 309-16.
11. Sjoback, R.; Nygren, J.; Kubista, M. Absorption and Fluorescence Properties of Fluorescein. *Spectrochimica Acta Part a-Molecular and Biomolecular Spectroscopy* **1995**, *51* (6), L7-L21.
12. Maeda, T.; Nagahara, T.; Aida, M.; Ishibashi, T. Identification of chemical species of fluorescein isothiocyanate isomer-I (FITC) monolayers on platinum by doubly resonant sum-frequency generation spectroscopy. *Journal of Raman Spectroscopy* **2008**, *39* (11), 1694-1702.
13. Klonis, N.; Sawyer, W. H. Spectral properties of the prototropic forms of fluorescein in aqueous solution. *Journal of Fluorescence* **1996**, *6* (3), 147-57.
14. Mchedlov-Petrosyan, N.; Isaenko, Y. V.; Vodolazkaya, N. A.; Goga, S. T. Acid-Base Behavior of Fluorescein Isothiocyanate in Aqueous Media and in Micellar Surfactant Solutions (September 2003). *Chemistry Preprint Archive* **2003**, Vol. 2003 (9), 93-101.
15. Lakowicz, J. R. *Principles of Fluorescence Spectroscopy*; 3rd Edition ed.; Springer: New York, 2006.
16. Lok, B. K.; Cheng, Y.-L.; Robertson, C. R. Total internal reflection fluorescence: a technique for examining interactions of macromolecules with solid surfaces. *Journal of Colloid and Interface Science* **1983**, *91* (1), 87-103.
17. Welin-Klintström, S.; Wikström, M.; Askendal, A.; Elwing, H.; Lundström, I.; Karlsson, J. O.; Renvert, S. Proteolytic degradation of fibrinogen layers adsorbed on hydrophilic and hydrophobic surfaces. *Colloids and surfaces* **1990**, *44*, 51-60.
18. Jonsson, U.; Ivarsson, B.; Lundstrom, I.; Berghem, L. Adsorption Behavior of Fibronectin on Well-Characterized Silica Surfaces. *J. Colloid Interface Sci.* **1982**, *90* (1), 148-163.
19. Bartell, F. E.; Zuidema, H. H. Wetting Characteristics of Solids of Low Surface Tension such as Talc, Waxes and Resins. *J. Am. Chem. Soc.* **1936**, *58* (8), 1449-1454.
20. Togashi, D. M.; Szczupak, B.; Ryder, A. G.; Calvet, A.; O'Loughlin, M. Investigating Tryptophan Quenching of Fluorescein Fluorescence under Protolytic Equilibrium. *The Journal of Physical Chemistry A* **2009**, *113* (12), 2757-2767.
21. Rockhold, S. A.; Quinn, R. D.; Vanwagenen, R. A.; Andrade, J. D.; Reichert, M. Total Internal-Reflection Fluorescence (TIRF) as a Quantitative Probe of Protein Adsorption. *J. Electroanal. Chem.* **1983**, *150* (1-2), 261-275.
22. Reichert, W. M. Evanescent Detection of Adsorbed Films - Assessment of Optical Considerations for Absorbance and Fluorescence Spectroscopy at the Crystal Solution and Polymer-Solution Interfaces. *Critical Reviews in Biocompatibility* **1989**, *5* (2), 173-205.

23. Sero, L.; Sanguinet, L.; Derbre, S.; Boury, F.; Brotons, G.; Dabos-Seignon, S.; Richomme, P.; Seraphin, D. Fluorescent Self-Assembled Mono layers of Umbelliferone: A Relationship between Contact Angle and Fluorescence. *Langmuir* **2013**, *29* (33), 10423-10431.
24. Togashi, D. M.; Szczupak, B.; Ryder, A. G.; Calvet, A.; O'Loughlin, M. Investigating Tryptophan Quenching of Fluorescein Fluorescence under Protolytic Equilibrium. *J. Phys. Chem. A* **2009**, *113* (12), 2757-2767.
25. Sendner, C.; Horinek, D.; Bocquet, L.; Netz, R. R. Interfacial Water at Hydrophobic and Hydrophilic Surfaces: Slip, Viscosity, and Diffusion. *Langmuir* **2009**, *25* (18), 10768-10781.
26. Vogler, E. A. Structure and reactivity of water at biomaterial surfaces. *Adv. Colloid Interface Sci.* **1998**, *74*, 69-117.
27. Mante, P. A.; Chen, C. C.; Wen, Y. C.; Chen, H. Y.; Yang, S. C.; Huang, Y. R.; Chen, I. J.; Chen, Y. W.; Gusev, V.; Chen, M. J.; Kuo, J. L.; Sheu, J. K.; Sun, C. K. Probing Hydrophilic Interface of Solid/Liquid-Water by Nanoultrasonics. *Scientific Reports* **2014**, *4*, 6.
28. Robeson, J. L.; Tilton, R. D. Effect of Concentration Quenching on Fluorescence Recovery after Photobleaching Measurements. *Biophys. J.* **1995**, *68* (5), 2145-2155.
29. Hungerford, G.; Benesch, J.; Mano, J. F.; Reis, R. L. Effect of the labelling ratio on the photophysics of fluorescein isothiocyanate (FITC) conjugated to bovine serum albumin. *Photochem Photobiol Sci* **2007**, *6* (2), 152-8.
30. Song, A. M.; Zhang, J. H.; Zhang, M. H.; Shen, T.; Tang, J. A. Spectral properties and structure of fluorescein and its alkyl derivatives in micelles. *Colloids and Surfaces a-Physicochemical and Engineering Aspects* **2000**, *167* (3), 253-262.
31. Imhof, A.; Megens, M.; Engelberts, J.; De Lang, D.; Sprik, R.; Vos, W. Spectroscopy of fluorescein (FITC) dyed colloidal silica spheres. *Journal of Physical Chemistry. B* **1999**, *103* (9), 1408-1415.
32. Song, L. L.; Hennink, E. J.; Young, I. T.; Tanke, H. J. Photobleaching Kinetics of Fluorescein in Quantitative Fluorescence Microscopy. *Biophys. J.* **1995**, *68* (6), 2588-2600.
33. Usui, Y.; Itoh, K.; Koizumi, M. Switch-Over of Mechanism of Primary Processes in Photo-Oxidation of Xanthene Dyes as Revealed by Oxygen Consumption Experiments. *Bull. Chem. Soc. Jpn.* **1965**, *38* (6), 1015-+.
34. Periasamy, N.; Bicknese, S.; Verkman, A. S. Reversible photobleaching of fluorescein conjugates in air-saturated viscous solutions: Singlet and triplet state quenching by tryptophan. *Photochem. Photobiol.* **1996**, *63* (3), 265-271.
35. Li, L. H.; Rao, G.; Lv, X. H.; Chen, R. X.; Cheng, X. F.; Wang, X. J.; Zeng, S. Q.; Liu, X. L. Chemical reactivation of fluorescein isothiocyanate immunofluorescence-labeled resin-embedded samples. *Journal of Biomedical Optics* **2018**, *23* (2), 4.
36. Ouberai, M. M.; Xu, K.; Welland, M. E. Effect of the interplay between protein and surface on the properties of adsorbed protein layers. *Biomaterials* **2014**, *35* (24), 6157-6163.
37. Lassen, B.; Malmsten, M. Competitive protein adsorption at plasma polymer surfaces. *J. Colloid Interface Sci.* **1997**, *186* (1), 9-16.
38. Lassen, B.; Malmsten, M. Structure of protein layers during competitive adsorption. *J. Colloid Interface Sci.* **1996**, *180* (2), 339-349.
39. Togashi, D. M.; Ryder, A. G. Assessing protein-surface interactions with a series of multi-labelled BSA using Fluorescence Lifetime Imaging-Förster Energy Resonance Transfer. *Biophys. Chem.* **2010**, *152* (1-3), 55-64.
40. Taborelli, M.; Eng, L.; Descouts, P.; Ranieri, J. P.; Bellamkonda, R.; Aebischer, P. Bovine Serum-Albumin Conformation on Methyl and Amine Functionalized Surfaces Compared by Scanning Force Microscopy. *Journal of Biomedical Materials Research* **1995**, *29* (6), 707-714.
41. Phan, H. T. M.; Bartelt-Hunt, S.; Rodenhausen, K. B.; Schubert, M.; Bartz, J. C. Investigation of Bovine Serum Albumin (BSA) Attachment onto Self-Assembled Monolayers (SAMs) Using Combinatorial Quartz Crystal Microbalance with Dissipation (QCM-D) and Spectroscopic Ellipsometry (SE). *Plos One* **2015**, *10* (10), 20.

42. Hasan, A.; Waibhaw, G.; Pandey, L. M. Conformational and Organizational Insights into Serum Proteins during Competitive Adsorption on Self-Assembled Monolayers. *Langmuir* **2018**, *34* (28), 8178-8194.
43. Sheller, N. B.; Petrash, S.; Foster, M. D.; Tsukruk, V. V. Atomic force microscopy and X-ray reflectivity studies of albumin adsorbed onto self-assembled monolayers of hexadecyltrichlorosilane. *Langmuir* **1998**, *14* (16), 4535-4544.
44. Nakanishi, K.; Sakiyama, T.; Imamura, K. On the adsorption of proteins on solid surfaces, a common but very complicated phenomenon. *J. Biosci. Bioeng.* **2001**, *91* (3), 233-244.
45. Panchuk-Voloshina, N.; Haugland, R. P.; Bishop-Stewart, J.; Bhalgat, M. K.; Millard, P. J.; Mao, F.; Leung, W. Y.; Haugland, R. P. Alexa dyes, a series of new fluorescent dyes that yield exceptionally bright, photostable conjugates. *Journal of Histochemistry & Cytochemistry* **1999**, *47* (9), 1179-1188.
46. Gajraj, A.; Ofoli, R. Y. Effect of extrinsic fluorescent labels on diffusion and adsorption kinetics of proteins at the liquid-liquid interface. *Langmuir* **2000**, *16* (21), 8085-8094.